

Earthquakes as dynamic fracture phenomena

Commentary by

Ze'ev Reches, University of Oklahoma, and Jay Fineberg, Hebrew University

ABSTRACT

A large earthquake unlocks a fault-zone via dynamic rupture while releasing part of the elastic energy stored during the interseismic stage. As earthquakes occur at depth, the analyses of earthquake physics rely primarily on experimental observations and conceptual models. A common view is that the earthquake instability is necessarily related to the frictional weakening that is commonly observed in shear experiments under seismic slip velocities. However, recent experiments with frictional interfaces in brittle acrylics (Svetlizky & Fineberg, 2014) and rocks (e.g., Passelegue et al., 2020) have explicitly demonstrated that no characteristic frictional strength exists; a wide range of stresses (‘overstresses’) are sustained prior to rupture nucleation. Moreover, the experimentally observed singular stress-fields and rupture dynamics are *precisely* those predicted by fracture mechanics (Freund, 1998). We therefore argue here that earthquake dynamics are best understood in terms of dynamic fracture mechanics; rupture dynamics are driven by overstresses, but not directly related to the fault frictional properties.

PLAIN-LANGUAGE SUMMARY

A large earthquake occurs when a “locked” fault becomes unlocked and starts slipping rapidly while releasing stored elastic energy. As earthquakes occur at depth, earthquake analyses rely primarily on experimental observations and conceptual models. One common view attributes the earthquake instability to the transition from the strong ‘static friction’ to the weaker ‘dynamic friction’. Recent observations of experimental earthquakes along brittle faults cause us to challenge this common view. These experiments have explicitly demonstrated that faults may stay locked under a wide range of stress levels making the assumption of a characteristic ‘static friction’ irrelevant. Moreover, the features of these earthquakes fit *precisely* the predictions of fracture mechanics theory (Freund, 1998), by taking these stress differences into account. We therefore argue here that earthquake dynamics is best understood in terms of dynamic fracture mechanics, a process not directly related to the fault frictional properties.

INTRODUCTION

A large earthquake is preceded by an interseismic period during which the fault-zone stays “locked”, and elastic energy is “stored” in the crustal rocks. The earthquake will unlock the fault-zone via dynamic rupture of the fault while releasing part of the stored elastic energy. Earthquake physics analyses rely primarily on experimental observations and conceptual models, because we have “.....near zero direct constraints on the dynamic processes ... associated with ... earthquake ruptures” (Ben-Zion, 2019). In this commentary, we examine the rupture character

37 of earthquakes in light of recent experimental observations; we start by inspecting the earthquake
38 process in the framework of dynamic fracturing.

39 Figure 1 displays three idealized cases of dynamic fracturing: tensile fracturing (mode I),
40 shear fracturing without friction (mode II), and shear fracturing along a frictional fault, that is an
41 idealized earthquake rupture. The processes of tensile and shear fracturing (modes I and II) have
42 been under detailed investigation since (Griffith, 1920) and are well understood by the theory of
43 ‘fracture mechanics’ (Freund, 1998). This theory indicates that both tensile and shear fractures
44 will propagate when the rate of elastic energy flow towards the tip of a rapidly moving fracture
45 surpasses the rate of local energy dissipation required for creating the new fracture surfaces
46 (Freund, 1998; Svetlizky et al., 2017). In modes I and II, resulting fractured surfaces (white slits
47 in Fig. 1a, b) are stress-free, and thus, the only site where energy is dissipated is within the
48 fracture tip zone (yellow zone in Fig. 1a, b). Fracture mechanics theory provides analytical
49 solutions of the stress-field around the fracture as a function of the available energy and
50 propagation velocity. The predicted stress-field indicates a distinct stress singularity at the tip,
51 and a stress-free zone in the wake of the tip (dark blue zone of $\sigma = 0$ in Fig. 1d).

52 As anticipated, the situation becomes more complicated for a shear fracture in which both
53 sides of the fracture surfaces remain in frictional contact (Fig. 1c). This configuration is the
54 relevant one for an earthquake rupturing a frictional fault. Theoretical work (Barras et al., 2020;
55 Palmer & Rice, 1973) has suggested that even this case can, in general, be described by the same
56 fracture mechanical framework as the pure mode II case (Fig. 1b).

57

58 RUPTURING ALONG EXPERIMENTAL FRICTIONAL FAULTS

59 Recent experimental analyses use advanced high-speed techniques to monitor dynamic
60 ruptures along experimental faults (Svetlizky & Fineberg, 2014; Wu & McLaskey, 2019; Xu et
61 al., 2019; Passelegue et al., 2020; Xiaofeng Chen et al., 2021a). These analyses revealed three
62 fundamental characteristics of shear rupturing along frictional faults with significant implications
63 for earthquake physics.

64 I. **Stresses and control of dynamic rupturing.** It was demonstrated (Svetlizky & Fineberg,
65 2014) that propagating ruptures along a fault can be *precisely* described by fracture
66 mechanics theory (Freund, 1998). Fig. 2 displays the results for an experimental fault (Fig.
67 2a) that was subjected to shear and normal loads where ruptures were monitored by high-
68 speed photography and strain-gages. In a series of nine experiments, the fault was
69 overstressed prior to rupture initiation over a range of shear stresses that exceeded the
70 minimal stress for frictional sliding (about 1MPa) by 0.1-0.4 MPa (the normal load was
71 identical in all experiments) (Fig. 2b). Once slip nucleated, spontaneous ruptures propagated
72 at velocities that were governed by the pre-slip overstress (Fig. 2c). The lowest overstress
73 triggered relatively slow ruptures, while the highest values gave rise to rapidly accelerating

74 ruptures that approached the limiting Raleigh wave speed, C_R . (Svetlizky et al., 2017) used
75 the measured elastic energy to show that all the propagation velocities and accelerations in
76 these experiments *perfectly* fit the fracture mechanics predictions (black curve in Fig. 2d).
77 Most importantly, this perfect fit does not include any consideration of the fault’s frictional
78 properties. These experimental observations are in agreement with fracture mechanics
79 formulations which indicated that fault friction does not affect the rupture characteristics
80 (Barras et al., 2020; Palmer & Rice, 1973). This quantitative agreement with fracture
81 mechanics theory, which was documented in both brittle acrylics (Svetlizky & Fineberg,
82 2014; Bayart et al., 2016; Svetlizky et al., 2017) and rocks (Wu & McLaskey, 2019; Xu et
83 al., 2019; Passelegue et al., 2020), requires a modification of the predicted stress-field; the
84 stress in the frictional zone equals the residual frictional strength of the fault, τ_R , (grey area
85 of $\sigma = \tau_R$, Fig. 1e).

86
87 **II. Energy balance of dynamic rupturing.** The section above indicates that the elastic
88 energy dissipation can be separated into two, quasi-independent entities (Fig. 1): (A)
89 Localized dissipation (fracture energy) at the near-singular tip zone of a shear fracture
90 (yellow zone, Fig. 1c), and (B) distributed energy dissipation by frictional resistance of the
91 sliding surfaces in the wake of the rupture-front (red fault-zone, Fig. 1c). The rupture front
92 may propagate at velocities of a few km/s (Fig. 2c) while generating extreme stresses,
93 strain-rates and slip velocities, in the immediate vicinity of rupture tip (Svetlizky &
94 Fineberg, 2014). The near-tip, cohesive zone of a typical earthquake dissipates only ~5-6%
95 of the earthquake energy (Kanamori & Brodsky, 2004), but the extreme stresses developed
96 there are expected to “breakdown” the fault-zone by fragmentation and pulverization (Chen
97 et al., 2021b; Reches & Dewers, 2005; Wilson et al., 2005). The trailing frictional zone,
98 which does not constrain the rupture front, is thought to dissipate 70-90% of the earthquake
99 energy. The above observations and associated discussion raise a central question: What are
100 the effects of *friction* on the earthquake process?

101
102 **III. Fault frictional properties and the earthquake process.** A common view is that
103 earthquake instability is controlled by frictional weakening manifested by the drop from static
104 to dynamic friction (Di Toro et al., 2011; Dieterich, 1979). This view is used in earthquake
105 simulations with velocity weakening (Lapusta & Rice, 2003; Madariaga et al., 1998)
106 assuming experimentally derived friction laws, e.g., rate-and-state friction (Dieterich, 1979).
107 Frictional weakening is indeed observed in multiple experiments; a rock’s frictional strength
108 may decrease with increasing slip-velocity and/or slip-displacement. Strengths drop
109 particularly rapidly under seismic slip velocities of a few m/s (Di Toro et al., 2011; Hirose &
110 Shimamoto, 2005). We argue that the utilization of frictional weakening as the controlling
111 mechanism of earthquake dynamics may lead to a few central contradictions.

112

113 Sections I and II above indicate that the dynamic nature (e.g., stored energy, stress field, or
114 propagation velocity) of a rupture along experimental faults can be fully understood in terms
115 of fracture mechanics formulation without consideration of the fault’s frictional properties.

116 The only requirement for earthquake rupture propagation is the ability of a frictional system to
117 develop and sustain sufficient stored elastic energy, or ‘overstress’, prior to rupture nucleation
118 (e.g. Fig. 2b). This has been amply demonstrated (Ben-David et al., 2010; Ben-David &
119 Fineberg, 2011; Passelegue et al., 2020) in experiments; for a given normal stress, an
120 experimental fault can sustain a large range of applied shear stresses. Therefore, the concept
121 of a characteristic static-friction that governs the onset of instability is misleading (Ben-David
122 & Fineberg, 2011), and a fault system can store varying amounts of elastic energy above
123 limits imposed by friction-based models; mechanisms of overstress are discussed later.

124 It is certainly possible to incorporate frictional weakening in rupture dynamics simulations
125 that correspond to fracture mechanics formulations (Lapusta & Rice, 2003; Madariaga et al.,
126 1998). However, the required dependence on a ‘friction law’ and associated weakening is *not*
127 *necessary*, and, in fact, could impose unnecessary restrictions. For example, the friction-based
128 idea that an earthquake cannot propagate under velocity *strengthening* is inaccurate, because
129 an earthquake can propagate if the fault system is sufficiently overstressed. For instance, the
130 mineral talc dominates the composition of active fault-zones, e.g., the central San Andreas
131 fault (Moore, D. & Rymer, M., 2007) and mining–induced faults. Yet, even though talc is
132 documented as frictional-strengthening mineral for both dynamic velocity and displacement
133 (XF Chen et al., 2017), earthquakes do occur along these zones.

134 DISCUSSION

135 We propose here that earthquakes should be described as dynamic ruptures controlled by
136 fracture mechanics processes that are unrelated to the friction even though fault frictional
137 properties do dominate the energy dissipation processes. We refer to this concept as Fracture
138 Earthquake Rupture Mechanics, FERM. Beyond the experimental observations, the proposed
139 view can resolve a few paradoxical features of earthquake processes.

140 **Overshoot** is a rupture state that can inherently be explained by the FERM concept.
141 Dynamic overshoot refers to the case of “...shear stress reduction below dynamic friction” (Ide
142 et al., 2011), and according to common friction laws, an earthquake should be arrested in such a
143 case. A field example of overshoot is the Mw2.2 earthquake at 3.6 km depth in Tautona mine,
144 South Africa. The in-situ mapping at the focal depth revealed a rupture-zone of 3 to 4 non-
145 parallel slip-surfaces (Heesakkers et al., 2011), and the associated in-situ stress measurements
146 (Lucier et al., 2009) revealed that the [shear stress/normal stress] ratio on these slip-surfaces
147 ranges 0.05-0.13. These measured stress ratios are significantly lower than the dynamic friction,
148 and according to FERM, this earthquake was facilitated solely by the of potential elastic energy
149 generated by mine operations regardless of the resolved shear stresses and fault-zone strength.

150 Overshoot has also been experimentally documented (Bayart et al., 2016) where rupture
151 propagation was shown to continue at stress levels well below measured values of τ_R .

152 **Overstress.** In FERM, the development of a dynamic rupture only requires a measure of
153 overstress, namely, mean stress levels that exceed those necessary to overcome τ_R . Overstress
154 can be achieved by a strong barrier (Gvirtsman & Fineberg, 2021), fault-zone healing
155 (Heesakkers et al., 2011; Muhuri et al., 2003) ahead of an arrested rupture (Ben-David et al.,
156 2010; Passelegue et al., 2020) or due to fault heterogeneities, whose strength may approach the
157 theoretical rock strength (Savage et al., 1996).

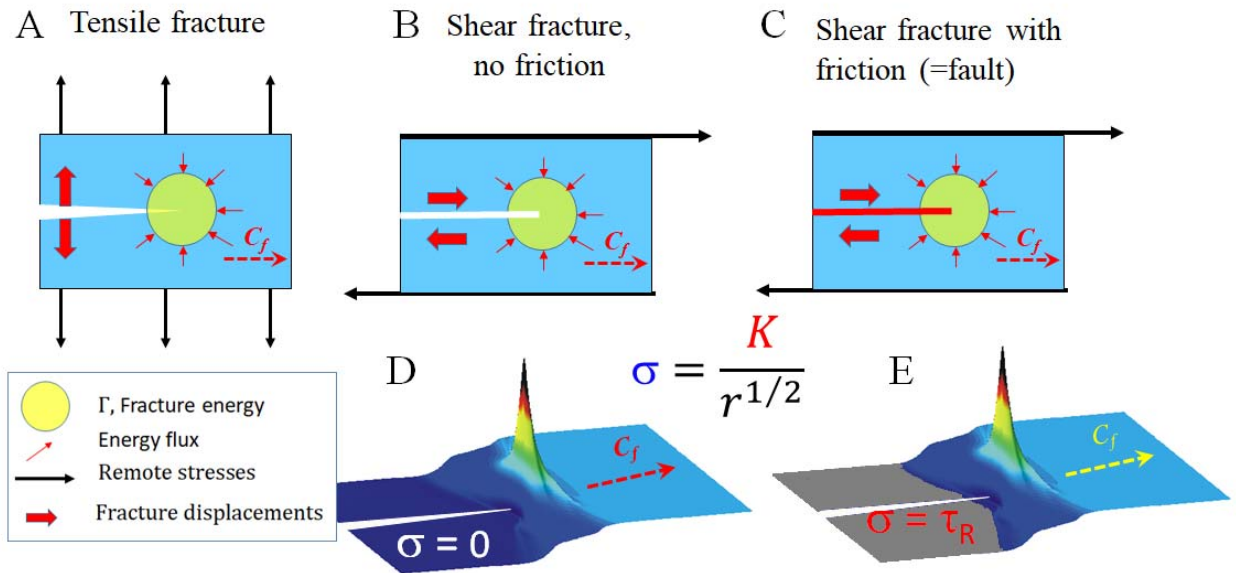
158 The stored elastic energy due to the overstress drives dynamic rupture and controls the
159 rupture velocity, style and energy dissipation after the rupture nucleation (Fig. 2) (Svetlizky et
160 al., 2017; Svetlizky & Fineberg, 2014). The timing and location of rupture nucleation are
161 governed by local failure in regions of high local stress and/or low local strength.

162 In conclusion, we believe that rupture fronts efficiently (~5% of the total energy) control
163 earthquake dynamics by unlocking a fault, generating the requisite breakdown stress-drop, and
164 damaging the rock-blocks. An earthquake's size and speed is controlled by the magnitude of the
165 elastic energy available relative to the interface strength (fracture energy), while the overall
166 dissipation is primarily due to frictional processes along slipping faults.

167 ACKNOWLEDGMENTS

168 We thank the many colleagues who through countless discussions unknowingly contributed
169 to our understanding of earthquake processes. ZR thanks the funding support by NSF grant
170 EAR-1620330 "Investigating earthquake source processes in the laboratory", and partial support
171 by NSF grant EAR-1345087 "Experimental simulation of earthquake rupture processes." JF
172 acknowledges the support of the Israel Science Foundation (ISF Grant No. 840/19). Open
173 Research and Data Availability: No unpublished data was used in this commentary.

174



176

177

178

179

180

181

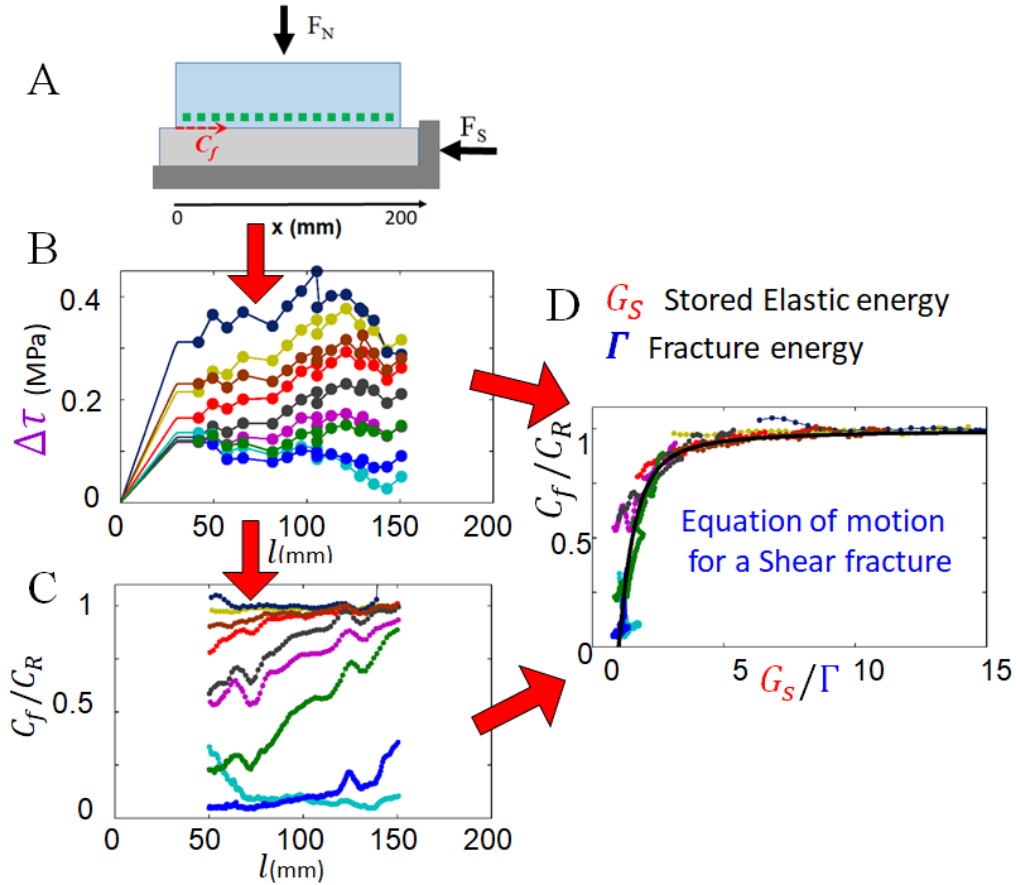
182

183

184

185

Figure 1: Schematic representations of (A) tensile (mode I) fracture, (B) shear fracture (mode II); in both A and B the crack faces formed behind the leading edge (crack tip) are stress-free. (C) Shear fracture with a frictional interface; a frictional residual shear stress, τ_R , remains in the wake of the fracture tip. In all three cases the elastic energy flowing into the tip is focused to a stress singularity of the form $\sigma = \frac{K}{r^{1/2}}$ where K is the stress-intensity factor and r is the distance from the tip. This stress-field is shown schematically in D (for cases A and B) and in E for case C.



186

187 *Figure 2:* Experimental rupture dynamics along a frictional fault. A, A schematic
 188 representation of an experimental system where two contacting acrylic blocks form a frictional
 189 interface. A normal force, F_N , (typically 3 MPa) is applied initially, then shear force, F_S , is
 190 increased quasi-statically until the development of stick-slip ruptures and frictional sliding. The
 191 rupture propagation velocity and strains are monitored by real-time measurements of the
 192 interface contact area with an optical method (Svetlizky & Fineberg, 2014), and a rapid
 193 measurements (1MHz rate) of the strain gauges (green squares). B. The measured shear stresses
 194 along the interface *prior to* rupture is presented for nine experiments conducted for identical
 195 values of F_N . The shown over-stresses, $\Delta\tau$, are the shear stress values in excess of the residual
 196 stress, τ_R , that is measured in the wake of the rupture front. For each of these stress profiles, a
 197 rupture was nucleated and propagated along the fault (Svetlizky et al., 2017). C. The rupture
 198 propagation velocity, C_f , and acceleration along the interface of the nine experiments in (B);
 199 shown the C_f normalize by the limiting wave speed, C_R for ruptures. D. Using the equation of
 200 motion (energy balance) predicted by fracture mechanics, all of the different velocity
 201 measurements collapse onto a single curve (black line) that depends on the ratio of the available
 202 elastic energy G_S and the fracture energy, Γ . Note that there are no adjustable parameters to the
 203 theory's predictions.

204

205 REFERENCES

- 206 Barras, F., Aldam, M., Roch, T., Brener, E., Bouchbinder, E., & Molinari, J. (2020). The
207 emergence of crack-like behavior of frictional rupture: Edge singularity and energy balance.
208 *Earth and Planetary Science Letters*, 531. <https://doi.org/10.1016/j.epsl.2019.115978>
- 209 Bayart, E., Svetlizky, I., & Fineberg, J. (2016). Fracture mechanics determine the lengths of
210 interface ruptures that mediate frictional motion. *Nature Physics*, 12(2), 166-170.
211 <https://doi.org/10.1038/NPHYS3539>
- 212 Ben-David, O., & Fineberg, J. (2011). Static Friction Coefficient Is Not a Material Constant.
213 *Physical Review Letters*, 106(25), 254301. <https://doi.org/10.1103/PhysRevLett.106.254301>
- 214 Ben-David, O., Cohen, G., & Fineberg, J. (2010). The Dynamics of the Onset of Frictional Slip.
215 *Science*, 330(6001), 211–214. <https://doi.org/10.1126/science.1194777>
- 216 Ben-Zion, Y. (2019). A Critical Data Gap in Earthquake Physics. *Seismological Research*
217 *Letters*, 90, 1721-1722 <https://doi.org/10.1785/0220190167>
- 218 Chen, X., Elwood Madden, A. S., & Reches, Z. (2017). The frictional strength of talc gouge in
219 high-velocity shear experiments. *J Geophysical Research: Solid Earth*, 122(5), 3661-3676.
- 220 Chen, X., Chitta, S. S., Zu, X., & Reches, Z. (2021). Dynamic fault weakening during
221 earthquakes: Rupture or friction? *Earth and Planetary Science Letters*, 575, 117165.
222 <https://doi.org/10.1016/j.epsl.2021.117165>
- 223 Di Toro, G., Han, R., Hirose, T., De Paola, N., Nielsen, S., Mizoguchi, K., et al. (2011). Fault
224 lubrication during earthquakes. *Nature*, 471(7339), 494-498.
- 225 Dieterich, J. H. (1979). Modeling of Rock Friction .1. Experimental Results and Constitutive
226 Equations. *J Geophysical Research*, 84(B5), 2161–2168.
- 227 Freund, L. B. (1998). *Dynamic fracture mechanics*. Cambridge university press.
- 228 Griffith, A. A. (1920). The phenomena of rupture and flow in solids. *Phil. Trans. Roy. Soc*,
229 A221, 163–198.
- 230 Gvirtsman, S., & Fineberg, J. (2021). Nucleation fronts ignite the interface rupture that initiates
231 frictional motion. *Nature Physics*, 17(9), 1037-1042. [https://doi.org/10.1038/s41567-021-](https://doi.org/10.1038/s41567-021-01299-9)
232 [01299-9](https://doi.org/10.1038/s41567-021-01299-9)
- 233 Heesakkers, V., Murphy, S. K., & Reches, Z. (2011). Earthquake Rupture at Focal Depth, Part I:
234 Structure and Rupture of the Pretorius Fault, TauTona Mine, South Africa. *Pure and*
235 *Applied Geophysics*, 168, 2395–2425.
- 236 Hirose, T., & Shimamoto, T. (2005). Growth of molten zone as a mechanism of slip weakening
237 of simulated faults in gabbro during frictional melting. *J Geophysical Research: Solid Earth*,
238 110(B5). <https://doi.org/10.1029/2004JB003207>

- 239 Ide, S., Baltay, A., & Beroza, G. C. (2011). Shallow Dynamic Overshoot and Energetic Deep
240 Rupture in the 2011 Mw 9.0 Tohoku-Oki Earthquake. *Science*, 332(6036), 1426–1429.
241 <https://doi.org/10.1126/science.1207020>
- 242 Kanamori, H., & Brodsky, E. E. (2004). The physics of earthquakes. *Reports on Progress in*
243 *Physics*, 67(8), 1429–1496.
- 244 Lapusta, N., & Rice, J. R. (2003). Nucleation and early seismic propagation of small and large
245 events in a crustal earthquake model. *J Geophysical Research-Solid Earth*, 108(B4), 2205.
- 246 Lucier, A. M., Zoback, M. D., Heesakkers, V., Reches, Z., & Murphy, S. K. (2009).
247 Constraining the far-field in situ stress state near a deep South African gold mine.
248 *International J Rock Mechanics and Mining Sciences*, 46(3), 555–567.
249 <https://doi.org/10.1016/j.ijrmms.2008.09.005>
- 250 Madariaga, R., Olsen, K., & Archuleta, R. (1998). Modeling dynamic rupture in a 3D earthquake
251 fault model. *Bulletin of the Seismological Society of America*, 88(5), 1182–1197.
- 252 Moore, D. & Rymer, M. (2007). Talc-bearing serpentinite and the creeping section of the San
253 Andreas fault. *Nature*, 448, 795–797.
- 254 Muhuri, S. K., Dewers, T. A., Scott, T. E., & Reches, Z. (2003). Interseismic fault strengthening
255 and earthquake-slip instability: Friction or cohesion? *Geology*, 31, 881–884.
- 256 Palmer, A., C., & Rice, J., R. (1973). The Growth of Slip Surfaces in the Progressive Failure of
257 Over-Consolidated Clay. *Proceedings of The Royal Society A: Mathematical, Physical and*
258 *Engineering Sciences*, 332(1591 DO–10.1098/rspa.1973.0040), 527–548.
- 259 Passelegue, F. X., Almakari, M., Dublanchet, P., Barras, F., Fortin, J., & Violay, M. (2020).
260 Initial effective stress controls the nature of earthquakes. *Nature Communications*, 11(1), 1-
261 8. <https://doi.org/10.1038/s41467-020-18937-0>
- 262 Reches, Z., & Dewers, T. A. (2005). Gouge formation by dynamic pulverization during
263 earthquake rupture. *Earth and Planetary Science Letters*, 235(1), 361–374.
264 <https://doi.org/10.1016/j.epsl.2005.04.009>
- 265 Savage, J. C., Byerlee, J. D., & Lockner, D. A. (1996). Is internal friction friction? *Geophysical*
266 *Research Letters*, 23(5), 487–490. <https://doi.org/10.1029/96GL00241>
- 267 Svetlizky, I., & Fineberg, J. (2014). Classical shear cracks drive the onset of dry frictional
268 motion. *Nature*, 509(7499), 205-208. <https://doi.org/10.1038/nature13202>
- 269 Svetlizky, I., Kammer, D. S., Bayart, E., Cohen, G., & Fineberg, J. (2017). Brittle Fracture
270 Theory Predicts the Equation of Motion of Frictional Rupture Fronts. *Physical Review*
271 *Letters*, 118(12), 125501. <https://doi.org/10.1103/PhysRevLett.118.125501>
- 272 Wilson, B., Dewers, T., Reches, Z., & Brune, J. (2005). Particle size and energetics of gouge
273 from earthquake rupture zones. *Nature*, 434(7034), 749-752.
274 <https://doi.org/10.1038/nature03433>

- 275 Wu, B. S., & McLaskey, G. C. (2019). Contained Laboratory Earthquakes Ranging From Slow
276 to Fast. *J Geophysical Research-Solid Earth*, 124(10), 10270–10291.
277 <https://doi.org/10.1029/2019JB017865>
- 278 Xu, S., Fukuyama, E., & Yamashita, F. (2019). Robust Estimation of Rupture Properties at
279 Propagating Front of Laboratory Earthquakes. *J Geophysical Research-Solid Earth*, 124(1),
280 766-787. <https://doi.org/10.1029/2018JB016797>
- 281